RCS Reduction and Radiation Improvement of a Circularly Polarized Patch Antenna using AMC Structures

Wei Song*, Wen-Bo Zheng, Zi-Jian Han, and Xin-Qing Sheng

Center for Electromagnetic Simulation, School of Information and Electronics
Beijing Institute of Technology, Beijing, 100081, China
*wsong@bit.edu.cn

Abstract ─ Based on a polarization-dependent artificial magnetic conductor (AMC), a windmill-formed reflector is designed and applied to a circularly polarized patch antenna to reduce the radar cross section (RCS) and to improve the radiation properties of the antenna at the same time. Simulation and measurement results show that the proposed antenna bears an in-band RCS reduction for 10dB over a bandwidth of 30% for both polarizations. The 3dB axial ratio (AR) bandwidth is extended largely with gain improved compared with the reference antenna.

Index Terms ─ Artificial magnetic conductor (AMC), axial ratio (AR), circularly polarized (CP) antenna, radar cross section (RCS).

I. INTRODUCTION

Patch antennas have been widely used because of their advantages such as low profile, lightweight, low cost and easy fabrication [1]. With the development of aerospace technology and radar technology, the circularly polarized (CP) patch antenna is frequently applied in the field of electronic reconnaissance interference, wireless communication and GPS navigation [2-5].

Currently, many works can be found on CP patch antennas aiming at improving their radiation performances. Fabry-Perot (FP) cavity is often used for high-gain CP antenna designs [6-10]. Metasurface superstrates are incorporated on CP patch antennas [6, 8, 9], or CP patch antenna array [10]. In [6, 9], not only the FP cavity is formed between the superstrate and the ground of the antenna, but also the stopband property of the EBG superstrate prohibits the radiation of side lobes. As a result, the front gain is improved largely. In [8] and [10], with surface waves on the metasurface excited, extra resonances with minimum AR points are produced. Consequently, the impedance bandwidth, the AR bandwidths and the gain of the antennas are all improved. There is also effort in designing a wideband high-gain CP antenna by using a single dielectric superstrate [7]. The superstrate not only enhances the gain attributed to the FP cavity formed, but also generates extra CP radiation for the system, and consequently broadens the AR bandwidth significantly. In [11, 12], through polarization conversion metasurfaces, linearly polarized waves are converted into CP ones and thus CP antennas with wider impedance bandwidth and higher gain are developed.

However, for CP patch antennas, there are only a few studies devoted to reducing the RCS of the antennas. Circular [13] and quasi fractal [14] structures are etched on the ground of the CP patch antennas to reduce the RCSs of the CP antennas while maintaining their radiation performance. In an integrated structure, the antenna in [15] can possess the absorbing characteristic and the partially reflective characteristic simultaneously. The upper surface of the superstrate absorbs most of the incident wave by converting the electromagnetic (EM) wave into heat as Ohm loss to reduce the RCS of the antenna, while the bottom surface of the superstrate forms an FP resonance cavity to produce high directive gain. On the other hand, the artificial magnetic conductor made it feasible to design low RCS screen based on phase cancellation scheme [16]. Further, wideband property is enabled by adopting dual AMCs [17, 18]. Following such scheme, chessboard metasurfaces formed by dual polarization-dependent AMC (PD-AMC) is utilized to design low-RCS and high-gain CP antennas in [19, 20]. In both designs, the gain enhancement is obtained by using FP cavities, while the low-RCS feature is realized by phase cancellation from blocks of the chessboard metasurfaces. In [20] the AR is also improved by the metasurface. However, such CP antennas require certain thickness due to the requirement in forming a Fabry-Perot cavity.

In this paper, by incorporating a muti-functional metasurface, we propose a thin circularly polarized patch antenna with properties of low RCS, high gain and broader AR bandwidth. In this design, PD-AMCs arranged in windmill-form [21] is used to construct a low RCS reflector. By forming the windmill patterned reflector with triangular topology of the AMCs, the number of the interfaces is increased. Consequently, such configuration directs the EM scattering to a wider

Submitted On: March 7, 2019
Accepted On: June 1, 2019

angular range compared with the traditional chessboard reflector. The very windmill-form metasurface, instead of an FP cavity as in literatures [15, 19, 20], also works as parametric radiating parts for the CP antenna which provides gain improvement. Wider AR bandwidth can be obtained by rotating the key part of the AMC elements which are on the diagonal direction. The windmill-form pattern for the reflector shows a second benefit that minor destruction is resulted in the low RCS performance when the aforementioned elements rotation is introduced. The performance of the proposed antenna, including a low RCS, broader 3-dB AR bandwidths, and enhanced gain, have been demonstrated by simulation and by experiments. The ANSYS High-Frequency Structure Simulator (HFSS) is used throughout this work for simulations.

II. DESIGN OF ANTENNA WITH WINDMILL-FORMED REFLECTOR

A. Design of the unit cell and windmill-formed reflector

In this paper, a mushroom-like AMC is designed on a substrate with thickness of 2mm and dielectric constant of 2.2. As shown in Fig. 1, parameters of the unit cell are as follows: P = 10.6mm, L = 8.9mm, W = 6.4mm, h = 2mm, r = 0.5mm, $g1$ = 2.1mm, and $g2$ = 0.85mm. By rotating this AMC (AMC1) by 90 degrees, we obtain another AMC (AMC2) with different reflection phase property. The reflection phases of these two AMCs were obtained by HFSS software, with the master and slave boundary and the Floquet port shown in Fig. 2 (a). The phase difference of the two AMCs is plotted in Fig. 2 (b). According to [20], a low RCS reflector designed by phase cancelation scheme requires two kind of blocks with phase difference in the range of 180 ± 30º. With such a criterion, it can be checked in Fig. 2 (b) that the operating frequency band for these PD-AMCs is 8.8 GHz -10.8 GHz.

By assembling these PD-AMCs in triangular blocks based on an even-area strategy, a windmill-shaped reflector is formed, as shown in Fig. 3 (a). The monostatic RCS of this reflector for normal incidence of the x- and y-polarizations has been simulated. Referenced by that of a metallic board with the same size, the RCS reduction by this reflector is presented in Fig. 3 (b). From careful observation of Fig. 3 (a), it can be found that this windmill-formed structure is not rigorously x-y symmetrical. That is why this structure shows different RCS curves for different polarizations. Taking the RCS reduction of -10 dB as the criteria, the proposed windmill-formed reflector shows an RCS reduction band from 7.56 GHz to 11 GHz for x-polarization and 8.31 GHz to 11.13 GHz for y-polarization. The maximum RCS reduction around -25.7 dB is obtained at 8.05 GHz. The scattering pattern for x-polarization at this frequency is plotted in Fig. 4. It can be seen that the dominant EM energy is reflected from backward direction to ($\theta = 30º$, $\varphi = 28º$) and (θ = 30º, φ = 208º), which is a typical signature for reflector designed by phase cancellation scheme. Similar scattering pattern can be observed for y-polarization.

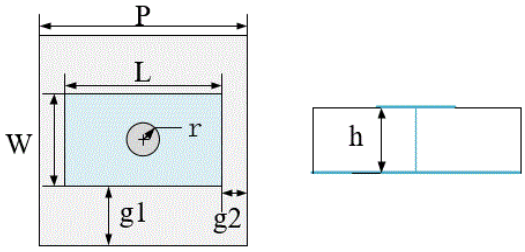

Fig. 1. The structure of AMC unit cell.

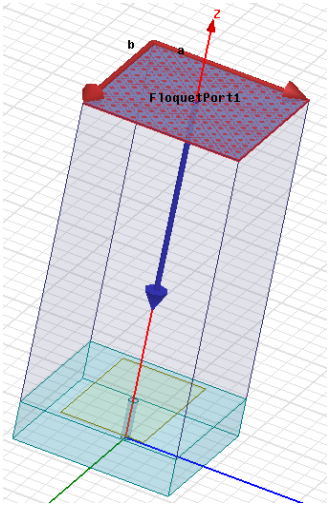

(a)

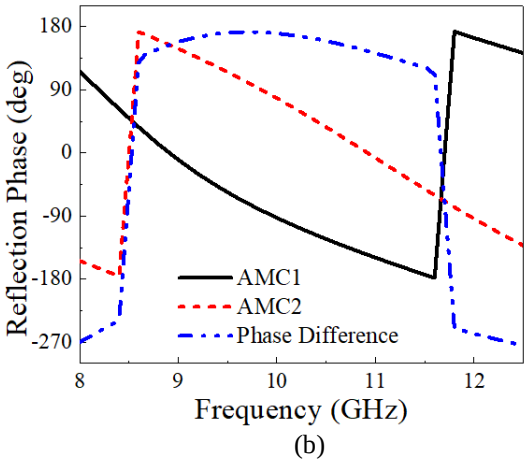

(b)

Fig. 2. (a) Simulation model of the AMC in HFSS, and (b) the reflection phase and phase difference of the two AMCs.

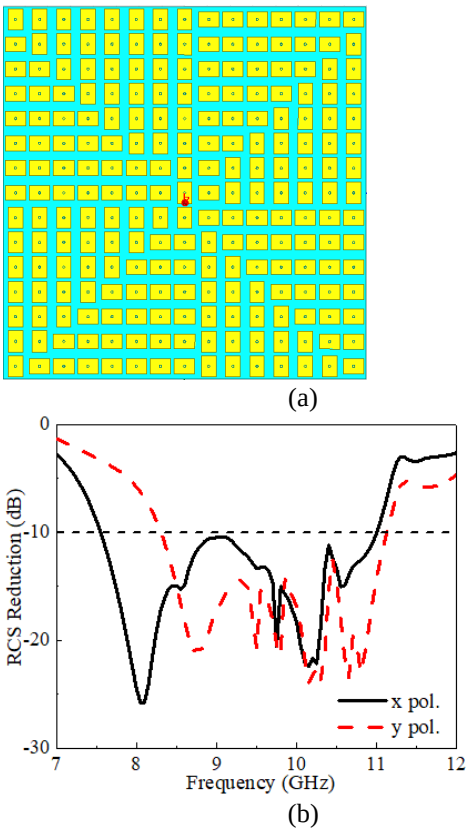

Fig. 3. (a) Illustration of the windmill-formed reflector, and (b) the simulated monostatic RCS of the windmill-formed reflector for normal incidences.

B. Design of the proposed antenna

In this section, the windmill-form reflector designed in section A is applied to a circularly polarized antenna. Based on a rectangular patch of 10*mm*×8.7*mm*, two isosceles right-angled triangles are cut from the central patch of the CP antenna [20], with details provided in Fig. 5 (a). The substrate is with dimension 159*mm*× 159*mm*×2*mm*. On top of the substrate, the windmill-formed reflector is applied surrounding the CP patch with a few modifications, as presented in Fig. 5 (b). Firstly, strong mutual coupling of the CP patch with its immediate neighboring AMCs will cause radiation degradation. Therefore, those AMC cells are removed to decrease this type of coupling. Secondly, the remaining central AMC elements dominantly work as parasitic radiating sources due to their coupling with the CP antennas [22], which enhances the gain of the patch. It is found by simulation that the axial ratio of the antenna is more sensitive to the currents on the diagonal direction of the substrate on which corners of the patch are cut. So a few centering AMC elements on this diagonal direction are rotated in order to adjust the induced x- and y-polarized currents. In this way, the AR bandwidth is obviously improved without violating the overall phase cancellation mechanism of the reflector when working in the scattering mode. After optimization, a rotation angle of 30º is obtained for this design to balance the multifunction of high gain, broad AR bandwidth, and low RCS of the antenna.

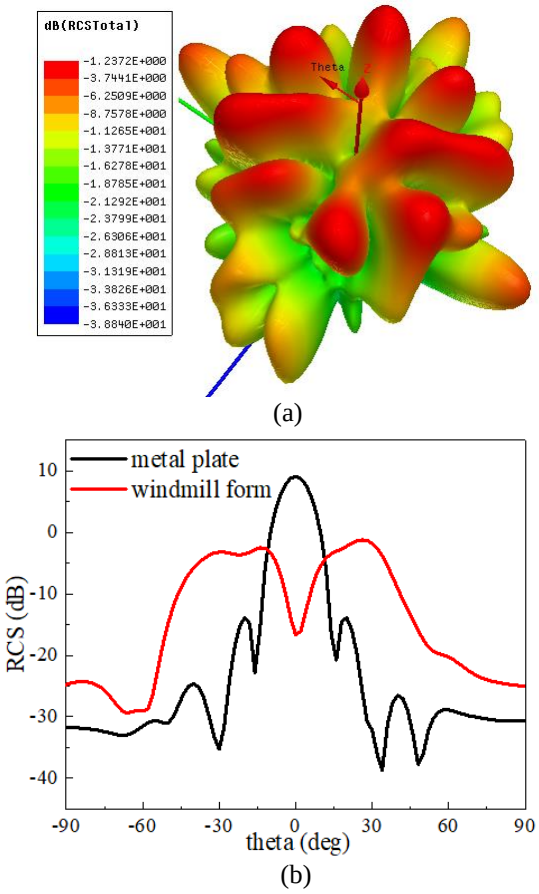

Fig. 4. The RCS pattern for the windmill-formed reflector at 8.05 GHz: (a) The 3-D pattern, and (b) the θ = 30º plane referenced by a metallic plate of the same size.

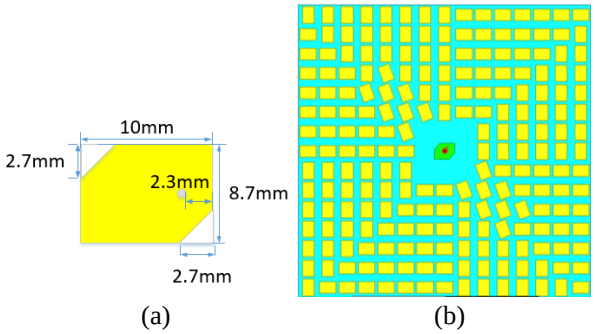

Fig. 5. Designs of: (a) the CP patch and (b) the proposed antennas.

Following the convention of [16, 17, 19, 20], the same CP antenna whose substrate is of the same size with the proposed antenna, is used as the reference antenna.

III. RESULTS AND DISCUSSION

A. Simulated radiation properties of the proposed antenna

Firstly, the radiation performance of the proposed antenna is examined by simulations. As shown in Fig. 6, the reference and the proposed CP antennas show almost the same impedance bandwidths (S_{11} < -10 dB) of 9.19 GHz - 11.3 GHz and 9.18 GHz - 11.34 GHz (21.1%). However, the bandwidth for 3dB AR of the main beam is extended from 9.91 GHz - 10.34 GHz (4.2%), to 9.86 GHz - 10.41 GHz (5.43%) by the proposed antenna, which means 29.3% increment in the AR bandwidth.

As shown in Fig. 7 (a), in the AR band, the gain of the reference antenna varies between 6.66 dB - 7.34 dB. In comparison, the proposed antenna yields a gain between 7.78 dB - 9.42 dB in its AR band. The gain enhancement is generally over 1 dB in the 3dB AR band, with a maximum of 2.44 dB at 10.1 GHz and minimum of 0.67 dB at 10.25 GHz.

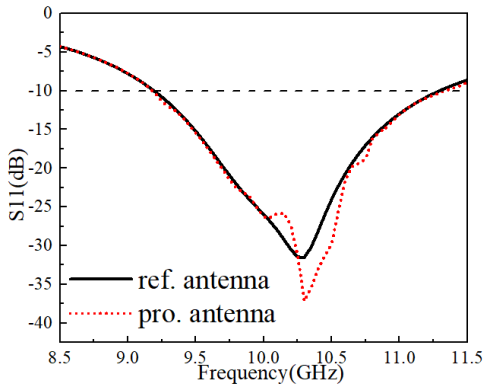

Fig. 6. (a) The impedance bandwidth, and (b) the AR bandwidth of the proposed and the reference antennas.

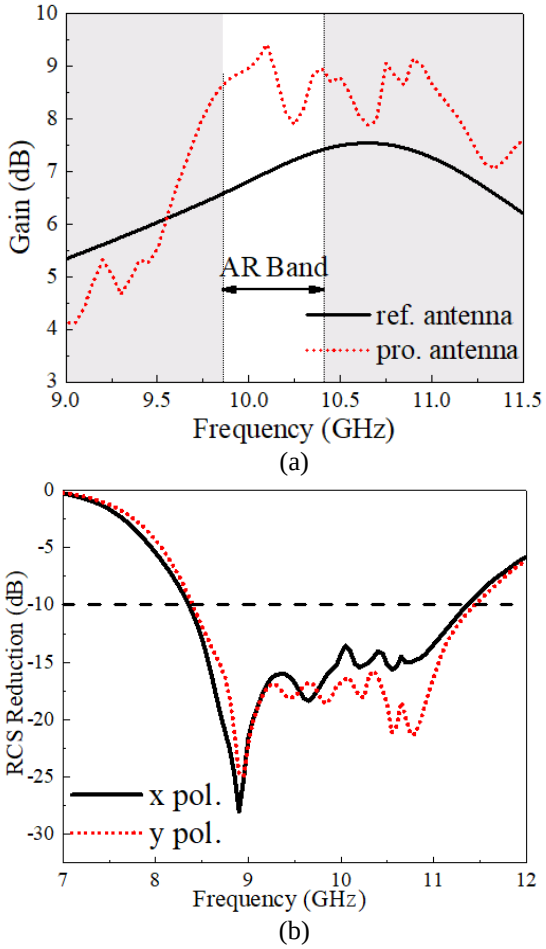

Fig. 7. (a) Gain of the proposed antenna and reference antenna, and (b) the RCS reduction of the proposed antenna for x- and y-polarized normal incidents.

B. RCS reduction of the proposed antenna

The monostatic RCS of the proposed and reference antennas for x-polarized and y-polarized normal incidents is also numerically investigated and the results are presented in Fig. 7 (b). It can be seen that, the proposed antenna with windmill-formed configuration shows an RCS reduction by more than 10 dB in a wideband frequency ranges from 8.35 GHz to 11.34 GHz (30.4% relative bandwidth) for x-x polarization. For y-y polarization, the 10dB RCS reduction frequency band is from 8.4 GHz to 11.4 GHz (30.3% relative bandwidth). Within the above bands, the maximum RCS reduction reaches 25.7 dB and 23 dB for x-x and y-y polarizations respectively. The operating band of the proposed antenna (9.91 GHz - 10.34 GHz) is covered by the RCS reduction band, which indicates an in-band RCS reduction is obtained. Compared with the similar work in [19, 20], the 3dB AR bandwidth is improved in this design, with detailed comparison listed in Table 1.

Table 1: Comparison of the AR bandwidth and RCS reduction

	AR 3dB-Bandwidth of CP Antenna	AR 3dB-Bandwidth of Improved CP Antenna	10dB-Bandwidth of RCS Reduction
Ref. [19]	5.87-6.07GHz (3.35%)	5.93-6.07GHz (2.3%)	13-15GHz (14.3%)
Ref. [20]	10.95-11.35GHz (3.6%)	10.45-11.85GHz (12.56%)	-
This paper	9.91-10.34GHz (4.2%)	9.86-10.41GHz (5.43%)	8.35-11.34GHz (30.4%)

C. Measurement results of the proposed antenna

The proposed antenna and the reference antenna were fabricated, with photos shown in Fig. 8. The setup in the anechoic chamber for measurement is shown in Fig. 9. The measurement results of S_{11} agree well with the simulation results, as shown in Fig. 10 (a). With regard to the axial ratio, as shown in Fig. 10 (b), the bandwidths are wider in measurement than in the simulation. The 3 dB AR band of the main beam is 9.9 GHz - 10.3 GHz for the reference antenna, with a bandwidth of 3.96%; while that for the proposed antenna is 9.8 GHz - 10.4 GHz, corresponding to a relative bandwidth of 5.94%. In other words, 50% expansion of the AR bandwidth is obtained in the measurement.

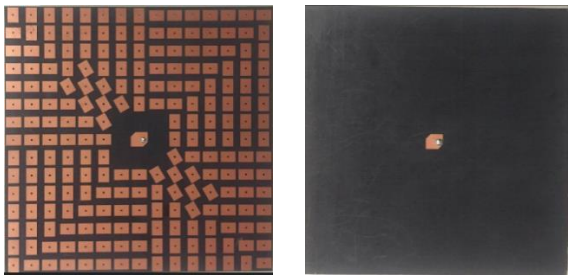

(a) (b)

Fig. 8. The photos of: (a) the proposed antenna and (b) the reference antenna.

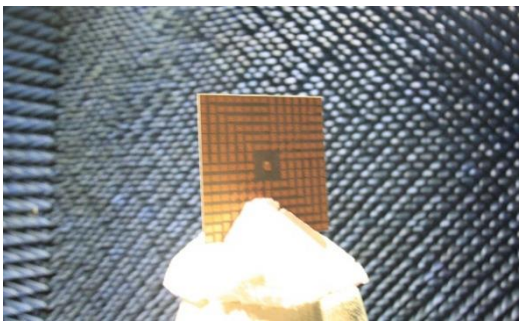

Fig. 9. Measurement setup in anechoic chamber.

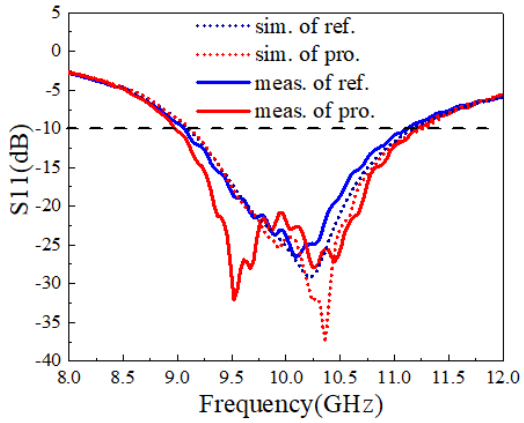

(a)

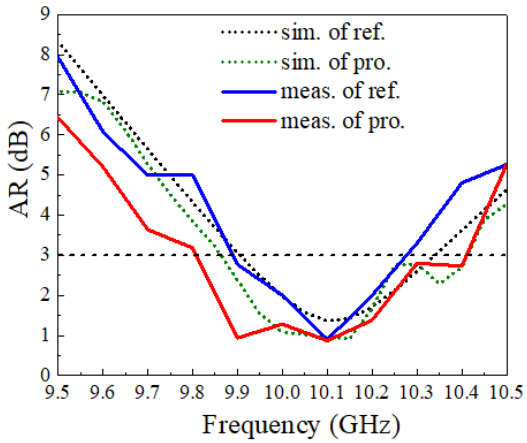

(b)

Fig. 10. (a) The S11 and (b) the AR of the proposed antenna and reference antenna.

The measured antenna gain is provided in Fig. 11 (a), in which improvement can be seen in the proposed antenna. The variation of the gain in the above AR band is below 3dB. As plotted in Fig. 11 (b), the measured radiation patterns agree well with those from the simulations. The fast changes in measured gain and the wider AR bandwidth could be attributed to the fabrication and measurement tolerance.

The monostatic RCSs of these antennas are measured from 8 GHz to 12 GHz and the results are provided in Fig. 12. An evident RCS reduction is seen for the vertical (corresponding to the x-x polarization in simulation due to the experimental set up) and the horizontal polarization (corresponding to y-y polarization in simulation). To be specific, 10 dB RCS reduction is obtained in frequency band of 8.6 GHz - 12.4 GHz, corresponding to a relative bandwidth of 32.6% for x-x polarization. The 10 dB RCS reduction band for y-y polarization is from 8.73 GHz to 11.95 GHz, with a relative bandwidth of 31.1%. The measured results of the RCS reduction generally agree with the simulations

except that the operating band for RCS reduction in measurement shifts upwards by nearly 1 GHz. This frequency shift may also be due to the fabrication tolerance. Despite of this frequency shift, the operating band of the proposed antenna is still covered by the RCS reduction band.

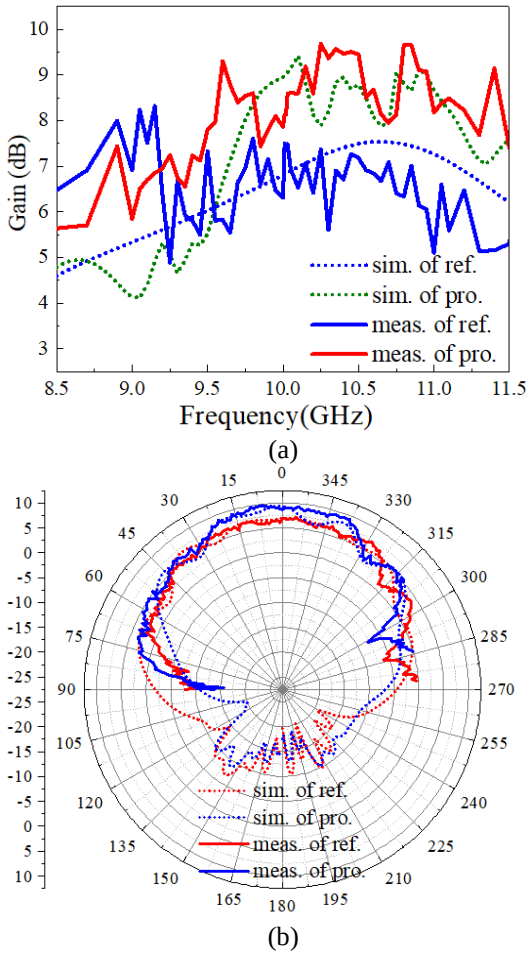

Fig. 11. (a) The gain and (b) the radiation patterns of the proposed and the reference antennas at 10GHz.

IV. CONCLUSION

In this paper, an in-band RCS reduction of the CP patch antenna is obtained by applying a modified windmill-formed configuration composed of PD-AMCs. By adopting windmill-formed reflector, backscatterings from different orientations of PD-AMCs cancel each other in the far field and lead to low RCS characteristics. It is verified by simulations and measurements that, 10 dB in-band RCS reduction is obtained with bandwidths of more than 30% for both x-x and y-y polarizations. By rotating some key AMC elements in the diagonal of the windmill-formed reflector, the axial ratio of the proposed antenna is improved. Referenced by the bare CP patch antenna, the experimental results show that the AR bandwidth of the proposed antenna is extended from 4.2% to 5.43% in simulation and from 3.96% to 5.94% in measurement. Gain improvement in the operating frequency band is also verified.

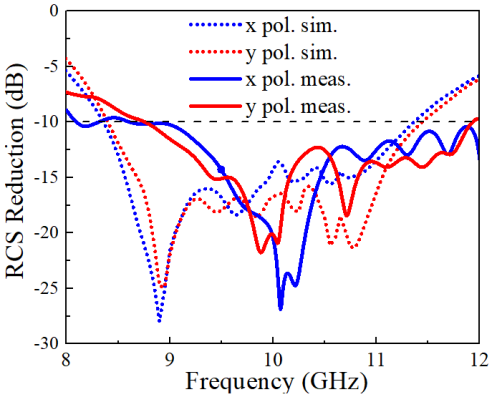

Fig. 12. Monostatic RCS of the proposed antenna and reference antenna.

ACKNOWLEDGMENT

This work is supported in part by the National Key R&D Program of China under Grant 2017YFB0202500, the NSFC under Grant Nos. 61601023 and U1730102.

REFERENCES

[1] K. F. Lee and K. F. Tong, "Microstrip patch antennas-basic characteristics and some recent advances," *Proc. IEEE*, vol. 100, no. 7, pp. 2169-2180, 2012.

[2] L. Sun, Y. H. Huang, and J. Y. Li, "A wideband circularly polarized candy-like patch antenna," *J. Electromagn. Waves Appl.*, vol. 25, no. 8, pp. 1113-1121, 2011.

[3] M. Ramírez and J. Parrón, "Dual-band circularly polarized microstrip antenna," *J. Electromagn. Waves Appl.*, vol. 26, no. 5, pp. 737-743, 2012.

[4] T. N. Chang and J. M. Lin, "Circularly polarized antenna having two linked slot-rings," *IEEE Trans. Antennas Propag.*, vol. 59, no. 8, pp. 3057-3060, 2011.

[5] A. A. Heidari, M. Heyrani, and M. Nakhkash, "A dual-band circularly polarized stub loaded microstrip patch antenna for GPS applications," *Progress in Electromagnetics Research.*, vol. 92, pp. 195-208, 2009.

[6] A. R. Vaidya, R. K. Gupta, and S. K. Mishra, "Right-hand/left-hand circularly polarized high-gain antennas using partially reflective surfaces," *IEEE Antennas Wireless Propag. Lett.*, vol. 13, pp. 431-434, 2014.

[7] S. X. Ta and T. K. Nguyen, "AR bandwidth and gain enhancements of patch antenna using single dielectric superstrate," *Electron. Lett.*, vol. 53, no.

15, pp. 1015-1017, 2017.

[8] K. L. Chung and S. Chaimool, "Diamagnetic metasurfaces for performance enhancement of microstrip patch antennas," *Proc. Eur. Conf. Antennas and Propagation (EUCAP)*, pp. 48-52, 2011.

[9] H. L. Dong, Y. J. Lee, J. Yeo, et al., "Directivity enhancement of circular polarized patch antenna using ring- shaped frequency selective surface superstrate," *Microwave Optical Techno Lett.*, vol. 49, no. 1, pp. 199-201, 2007.

[10] S. X. Ta and I. Park, "Compact wideband circularly polarized patch antenna array using metasurface," *IEEE Antennas Wireless Propag. Lett.*, vol. 16, pp. 1932-1936, 2017.

[11] H. L. Zhu, S. W. Cheung, and K. L. Chung, "Linear-to-circular polarization conversion using metasurface," *IEEE Trans. Antennas Propag.*, vol. 61, no. 9, pp. 4615-4623, 2013.

[12] Q. Zheng, C. Guo, and J. Ding, "Wideband and low RCS circularly polarized slot antenna based on polarization conversion of metasurface for satellite communication application," *Microwave Optical Techno Lett.*, vol. 60, no. 3, pp. 679-685, 2018.

[13] W. Jiang, Y. Zhang, and Z.-B. Deng, "Novel technique for RCS reduction of circularly polarized microstrip antennas," *J. Electromagn. Waves Appl.*, vol. 27, no. 9, pp. 1077-1088, 2013.

[14] W. Jiang, T. Hong, and S. X. Gong, "Research on the scattering characteristics and the RCS reduction of circularly polarized microstrip antenna," *International Journal of Antennas and Propaga.*, pp. 797-800, 2013.

[15] L. L. Cong, F. Qiang, X. Y. Cao, et al., "A novel circularly polarized patch antenna with low radar cross section and high-gain," *Acta Physica Sinica*, vol. 64, no. 22, 2015.

[16] M. Paquay, J. C. Iriarte, and I. Ederra, "Thin AMC structure for radar cross-section reduction," *IEEE Trans. Antennas Propag.*, vol. 55, no. 12, pp. 3630-3638, 2008.

[17] Y. J. Zheng, J. Gao, X. Y. Cao, et al., "A low radar cross-section artificial magnetic conductor reflection screen covering X and Ku band," *Acta Physica Sinica*, vol. 64, no. 2, pp. 24219-24219, 2015.

[18] J. C. I. Galarregui, A. T. Pereda, J. L. M. D. Falcón, I. Ederra, R. Gonzalo, and P. D. Maagt, "Broadband radar cross-section reduction using AMC technology," *IEEE Trans. Antennas Propag.*, vol. 61, no. 12, pp. 6136-6143, 2013.

[19] L. Zhang and T. Dong, "Low RCS and high-gain CP microstrip antenna using SA-MS," *Electron. Lett.*, vol. 53, no. 6, pp. 375-376, 2017.

[20] K. Li, Y. Liu, and Y. Jia, "A circularly polarized high-gain antenna with low RCS over a wideband using chessboard polarization conversion metasurface," *IEEE Trans. Antennas Propag.*, vol. 65, no. 8, 2017.

[21] Y. Zhang, R. Mittra, and B.-Z. Wang, "A novel design for low-RCS screens using a combination of dual-amc patches," *IEEE Antennas and Propagation Society International Symposium, Charleston, USA*, 2009.

[22] Z. J. Han, W. Song, and X. Q. Sheng, "Gain enhancement and RCS reduction for patch antenna by using polarization-dependent EBG surface," *IEEE Antennas & Wireless Propagation Letters*, vol. 16, pp. 1631-1634, 2017.

Wei Song obtained the Bachelor degree from the Northeastern University, China in 2002, and the M.Sc. and Ph.D. degrees in Queen Mary, University of London, U.K. in Electronic Engineering in 2003 and 2008 respectively. In 2008 she worked as a Postdoc Research Assistant in Antenna group, Queen Mary, University of London, and in the same year she joined the School of Information and Electronics at the Beijing Institute of Technology, where she is currently an Associate Professor.

Her research interests include computational electromagnetics, EM scattering analysis, antennas, and metamaterial analysis.

Wen-Bo Zheng was born in Shanxi, China in 1994. She received the Bachelor degree in Information and Electronic Engineering from Beijing Institute of Technology (BIT) in 2016. She is currently a graduate student in BIT.

Her main research interests are in the fields of antenna design, metasurface and Orbital Angular Momentum antenna.

Zijian Han was born in Liaoning, China in 1990. He graduated from Beijing Institute of Technology (BIT) in 2013. He started doing research as a Ph.D. student in BIT since 2013. He has already published SCI paper on IEEE AWPL and other EI papers.

His main research interests are in the fields of antenna design and metasurface.

Xin-Qing Sheng received his B.S., M.S., and Ph.D. degrees from the University of Science and Technology of China (USTC), Hefei, China, in 1991, 1994, and 1996, respectively. He is the Chang-Jiang Professor in the School of Information and Electronics, Beijing Institute of Technology, Beijing, China.